Int J Adv Manuf Technol (2017) 90:3543–3553
DOI 10.1007/s00170-016-9675-0

ORIGINAL ARTICLE

Design and optimization of non-circular mortar nozzles using finite volume method and Taguchi method

Min Zhou[1] · **Lingpan Kong**[1] · **Liangxi Xie**[1] · **Ting Fu**[1] · **Guozhang Jiang**[1] · **Qianmei Feng**[1,2]

Received: 7 July 2016 / Accepted: 28 October 2016 / Published online: 10 November 2016

Abstract The structure parameters of non-circular mortar nozzles for automatic wall-plastering machines are crucial in improving the performance of spraying uniformity and obtaining a larger plastering area, higher plastering quality, and efficiency. To address the non-uniformity issues of the existing mortar nozzles, we investigate the effects of a special nozzle structure on its outlet velocity uniformity by using Taguchi methods and the finite volume method. The experimental studies are conducted under various combinations of five factors: length, width, thickness, water-cement ratio, and inlet velocity, using a standard orthogonal array provided by Taguchi methods. The results reveal that the thickness, length, inlet velocity, width, and water-cement ratio are the influential factors on the outlet velocity uniformity. The interaction effects between length and thickness, length and width, and width and thickness are also significant on its outlet velocity uniformity. A higher water-cement ratio and a lower inlet velocity should be chosen as long as it meets the requirements of plastering quality and efficiency. The study of non-circular mortar nozzles provides an important reference for its systematic design in the future.

Keywords Non-circular mortar nozzles · Finite volume method · Taguchi method · Design and optimization

✉ Qianmei Feng
qmfeng@uh.edu

[1] College of Mechanical Automation, Wuhan University of Science and Technology, Wuhan, Hubei, China

[2] Department of Industrial Engineering, University of Houston, Houston, TX 77204, USA

1 Introduction

The construction of civil infrastructures is one of the oldest and largest economic sections that drive communities and nations. Comparing with current technological advancements, it is evident that the level of automation in construction is relatively low. It is a growing trend to advance technologies and automation in construction applications. Automatic wall-plastering machines have an exciting prospect in reducing the work intensity and shortening the project duration in the construction industry [1–4]. The structure parameters of mortar nozzles on the machines are crucial to ensure the performance and efficiency of wall-plastering machines. This paper focuses on the design and optimization of non-circular mortar nozzles for automatic wall-plastering machines. The optimized structure parameters of non-circular nozzles can enhance the spraying uniformity with a larger spraying area, leading to a higher plastering quality and efficiency.

In the construction industry, plastering of internal/external walls takes 20% of the overall construction duration. Plastering work not only is a heavy workload occupying a large amount of labor time but also has a low level of automation, which creates a bottleneck for the timely completion of a project. Automatic wall-plastering machines offer a great potential in reducing the work intensity and shortening the construction duration.

Mortar nozzles are one of the core components in automatic wall-plastering machines. Research on the nozzles has become the top priority in design of automatic wall plastering machines. Extensive research has been done on the performance of the nozzle. Ma and Zhang [5] observed that the diffusion angle and the

diffusion length of nozzles have a significant effect on the internal flow field of the nozzle, while the cylinder length of the nozzle has a low effect on it. Using numerical simulation of the internal flow field, they obtained the optimal parameter values of the nozzle. Yuan et al. tested both non-circular nozzles and circular nozzles with adjustable velocity, and they found that the former is more reliable compared with the latter in irrigation uniformity [6]; Kim et al. pointed out that the diffusion angle of the nozzle can affect its flow coefficient, which should be a focus in the design of micronozzles [7]. Long et al. put forward that the nozzle is one of the most important parts of jet pumps. Using numerical analysis, they found that the thickness of a nozzle tip can affect the nozzle flow field. The appropriate thickness should be chosen to enhance the performance of the jet pump [8].

The wall-plastering system with circular nozzles has been studied in the literature. The circular nozzles used in wall-plastering machines have features of a small plastering area, a thick center area, and a thin surrounding area [6]. For an automatic wall-plastering machine, however, the nozzle should have a sufficiently large plastering area, a high plastering velocity, and an even outlet velocity to meet the requirement of plastering efficiency and quality. Non-circular nozzles can potentially overcome the shortcomings presented in the traditional circular nozzles, which is more suitable for automatic wall-plastering machines.

This paper studies non-circular nozzles with a medium of mortar using the finite volume method and Taguchi methods. The nozzles with a medium of air, water, or oil have been studied in the literature in terms of the inner flow field, the outlet velocity value, and the energy loss [8–10]. This paper focuses on the medium of mortar and its resulting effects on non-circular nozzles. The finite volume method has been widely used as a numerical method in solving the fluid flow problems. A powerful computational fluid dynamics software, ANSYS Fluent, is used to simulate the distributions of velocity from various nozzle design schemes. While most existing research focuses on energy consumption, this research aims to study the influence of different parameters on the uniformity of nozzle outlet velocity, especially the complex interaction relationships of the nozzle structure parameters (the length, width, and thickness), the nozzle inlet velocity, and the water-cement ratio, using a standard orthogonal array provided by Taguchi methods. Taguchi methods are an effective tool in quality engineering, and its standard orthogonal arrays for experimental design can provide the full information of all the factors with a minimal number of experiments. Minitab software is used to assist analyzing the effects of different parameters and their interaction effects on the uniformity of nozzle outlet velocity. This study provides an important reference for the optimal design of non-circular nozzles.

The rest of this paper is organized as follows. In Sect. 2, the relevant mathematical models are provided. In Sect. 3, the details of experimental design by Taguchi methods and ANSYS Fluent simulation preparation are described. In Sect. 4, the results and analysis of ANSYS Fluent simulation and orthogonal tests are presented. In Sect. 5, conclusions and suggestions for parameter selections are provided.

2 Mathematical models for fluid dynamics

The methods for studying fluid motions include Lagrange method and Euler method. Lagrange method is mainly used to study the change of the position, velocity, other physical parameters of a selected fluid particle, and the historical process of the motion of a fluid particle in a period of time [11]. In the process of fluid motions, it is difficult to trace the motion of each particle, because the number of particles and the change of the particle positions are large in general. Therefore, Lagrange method is not suitable to be used to study the process of fluid motions.

Instead of directly studying the particle motion process, Euler method focuses on the whole flow field [12]. It studies the change rule of the particles in the flow field at different times. By observing the flow motion of each point in the space and its change with time, the whole motion of the fluid can be observed. At the same time, the velocity of each point in the space is different. At different times, a fixed point in the space is occupied by different fluid particles, and its velocity may be different as well. In practical applications, the motion parameters of fluid particles can be expressed by each point at each moment, leading to an easy understanding of the fluid motion. Therefore, the Euler method is used more extensively [13].

In conclusion, the velocity v is a function of the space coordinates (x, y, z) and the time t, or $v(x, y, z, t)$, which can be expressed as

$$v(x, y, z, t) = v_x(t)i + v_y(t)j + v_z(t)k \tag{1}$$

where $v_x(t)$, $v_y(t)$, and $v_z(t)$ are the velocity components of v in the x-direction, y-direction, and z-direction, respectively. Similarly, the pressure p and the density ρ are also functions of the space coordinates and the time, $p(x, y, z, t)$ and $\rho(x, y, z, t)$.

To study fluid motions using Euler method, we need to introduce the continuity equation, momentum equation, and energy equation, as described in Sects. 2.1, 2.2, and 2.3, respectively.

2.1 Continuity equation

In accordance with the law of mass conservation, the net fluid mass flowing in and out of a control volume should be equal to the reduced mass of the control volume within a certain unit of time. The differential form of the control equation of fluid flow can be derived as Eq. (2) [14]:

$$\frac{\partial \rho}{\partial t}+\frac{\partial(\rho u_x)}{\partial x}+\frac{\partial\left(\rho u_y\right)}{\partial y}+\frac{\partial(\rho u_z)}{\partial z}=0. \tag{2}$$

where $u_x, u_y,$ and u_z are velocity components in the x-direction, y-direction, and z-direction (m/s), respectively.

Using the Hamiltonian differential operator $\nabla = \mathrm{i}\frac{\partial \rho}{\partial x}+j\frac{\partial \rho}{\partial y}+k\frac{\partial \rho}{\partial z}$, the control equation of fluid flow in Eq. (2) can be expressed as Eq. (3):

$$\frac{\partial \rho}{\partial t}+\nabla\partial\cdot(\rho u)=0. \tag{3}$$

For the constant and incompressible fluid flow, $\frac{\partial \rho}{\partial t}=0$, Eq. (3) can be expressed as Eq. (4):

$$\frac{\partial u_x}{\partial x}+\frac{\partial u_y}{\partial y}+\frac{\partial u_z}{\partial z}=0. \tag{4}$$

2.2 Momentum equation

The essence of the fluid momentum equation is to satisfy Newton's second law: for a given fluid element, the momentum change rate with time is equal to the external force given to the element. According to the law, the momentum equations for the x-direction, y-direction, and z-direction can be derived as Eqs. (5), (6), and (7), respectively [14]:

$$\frac{\partial(\rho u_x)}{\partial t}+\nabla\cdot\left(\rho u_x\overrightarrow{u}\right)=-\frac{\partial p}{\partial x}+\frac{\partial \tau_{xx}}{\partial x}+\frac{\partial \tau_{yx}}{\partial y}+\frac{\partial \tau_{zx}}{\partial z}+\rho f_x \tag{5}$$

$$\frac{\partial\left(\rho u_y\right)}{\partial t}+\nabla\cdot\left(\rho u_y\overrightarrow{u}\right)=-\frac{\partial p}{\partial x}+\frac{\partial \tau_{xy}}{\partial x}+\frac{\partial \tau_{yy}}{\partial y}+\frac{\partial \tau_{zy}}{\partial z}+\rho f_y \tag{6}$$

$$\frac{\partial(\rho u_z)}{\partial t}+\nabla\cdot\left(\rho u_z\overrightarrow{u}\right)=-\frac{\partial p}{\partial x}+\frac{\partial \tau_{xz}}{\partial x}+\frac{\partial \tau_{yz}}{\partial y}+\frac{\partial \tau_{zz}}{\partial z}+\rho f_z \tag{7}$$

where p is the pressure of infinitesimal fluid element. $\tau_{xx}, \tau_{yx},$ and τ_{zx} are the components of the viscous stress τ, which is generated due to the molecular viscosity and has effects on the infinitesimal fluid element surface. f_x, f_y, and f_z are the force per unit mass in the three directions. If the infinitesimal fluid element is only forced by gravity and the z-axis is vertical, then $f_x=f_y=0$, and $f_z=-g$.

2.3 Energy equation

The energy equation of the fluid is the Bernoulli equation, the essence of which is the conservation of mechanical energy of the fluid. For having a steady flow when the viscous fluid flows along the pipe, the Bernoulli equation can be expressed as Eq. (8) [14]:

$$Z_1+\frac{p_1}{\rho g}+\frac{a_1V_1^2}{2g}=Z_2+\frac{p_2}{\rho g}+\frac{a_2V_2^2}{2g}+h_v \tag{8}$$

where Z is the potential energy of the unit weight relative to the reference level, which is also called the position head; $\frac{p}{\rho g}$ is the pressure energy for the unit mass, also called the pressure head; $\frac{aV^2}{2g}$ is for the kinetic energy of the unit weight of the fluid, also called the velocity head; a is the kinetic energy correction coefficient, and $a = 2$ for the circular tube laminar flow; V is the average flow velocity on the flow tube section; and h_v is energy loss of the unit weight along the flow process, which can be divided into the path loss and partial loss.

3 Experimental design and simulation preparation

The automatic wall-plastering machine designed in this paper aims to realize the function of automatic construction of mortar plastering with an efficiency of 100 m^2/h and a mortar thickness of 25 mm, i.e., the minimum amount of mortar needed to convey is 2.5 m^3/h. Considering the unexpected mortar falling in the plastering process, the output flow of mortar pump should be set at 4 m^3/h, and the inner diameter of the convey hose should be chosen as 50 mm. The nozzle structure is shown in Fig. 1. We need to analyze the influence of the factors (such as the nozzle structure, nozzle inlet velocity, and water-cement ratio) on the uniformity of the nozzle outlet velocity.

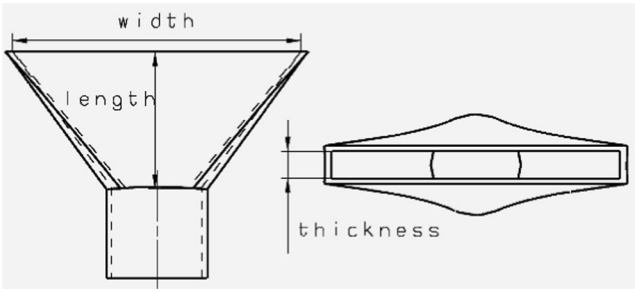

Fig. 1 Structure of non-circular nozzles

Table 1 Factors and levels of the orthogonal test

Level	Factor				
	A: length (mm)	B: width (mm)	C: thickness (mm)	D: water-cement ratio (dynamic viscosity Pa·s)	E: inlet velocity (m/s)
1	50	100	15	0.40 (0.090)	0.4448
2	100	150	20	0.45 (0.063)	0.5560
3	150	200	25	0.50 (0.037)	0.6672

3.1 Experimental design using Taguchi methods

As a key measure of the plastering quality of mortars [15–17], the uniformity of nozzle outlet velocity can be evaluated by the variance of the outlet velocity, i.e., a smaller variance of the velocity implies a higher degree of uniformity. To minimize the variance of the outlet velocity, an experimental design is an effective approach to analyze the influence of various factors on the variance of the velocity and select the optimal levels for different factors, namely, nozzle length, width, thickness, inlet velocity, and water-cement ratio. When the number of factors is large, however, a full factorial design results in a large number of experiments that have to be carried out. To reduce the number of experiments to a practical level, Taguchi methods using standard orthogonal arrays offer an efficient alternative that can provide the full information of all the factors with a minimal number of experiments [18].

We design a test scheme of five factors (i.e., nozzle length, width, thickness, inlet velocity, and water-cement ratio) and

Table 2 Layout of L_{27} orthogonal array for five factors

No.	Factor					The level of combination
	Length A (mm)	Width B (mm)	Thickness C (mm)	Water cement ratio D (dynamic viscosity Pa·s)	Inlet velocity (m/s)	
1	50	100	15	0.40 (0.090)	0.4448	$A_1B_1C_1D_1E_1$
2	50	100	15	0.40 (0.090)	0.5560	$A_1B_1C_1D_1E_2$
3	50	100	15	0.40 (0.090)	0.6672	$A_1B_1C_1D_1E_3$
4	50	150	20	0.45 (0.063)	0.4448	$A_1B_1C_2D_2E_1$
5	50	150	20	0.45 (0.063)	0.5560	$A_1B_2C_2D_2E_2$
6	50	150	20	0.45 (0.063)	0.6672	$A_1B_2C_2D_2E_3$
7	50	200	25	0.50 (0.037)	0.4448	$A_1B_3C_3D_3E_1$
8	50	200	25	0.50 (0.037)	0.5560	$A_1B_3C_3D_3E_2$
9	50	200	25	0.50 (0.037)	0.6672	$A_1B_3C_3D_3E_3$
10	100	100	20	0.50 (0.037)	0.4448	$A_2B_1C_2D_3E_1$
11	100	100	20	0.50 (0.037)	0.5560	$A_2B_1C_2D_3E_2$
12	100	100	20	0.50 (0.037)	0.6672	$A_2B_1C_2D_3E_3$
13	100	150	25	0.40 (0.090)	0.4448	$A_2B_2C_3D_1E_1$
14	100	150	25	0.40 (0.090)	0.5560	$A_2B_2C_3D_1E_2$
15	100	150	25	0.40 (0.090)	0.6672	$A_2B_2C_3D_1E_3$
16	100	200	15	0.45 (0.063)	0.4448	$A_2B_3C_1D_2E_1$
17	100	200	15	0.45 (0.063)	0.5560	$A_2B_3C_1D_2E_2$
18	100	200	15	0.45 (0.063)	0.6672	$A_2B_3C_1D_2E_3$
19	150	100	25	0.45 (0.063)	0.4448	$A_3B_1C_3D_2E_1$
20	150	100	25	0.45 (0.063)	0.5560	$A_3B_1C_3D_2E_2$
21	150	100	25	0.45 (0.063)	0.6672	$A_3B_1C_3D_2E_3$
22	150	150	15	0.50 (0.037)	0.4448	$A_3B_2C_1D_3E_1$
23	150	150	15	0.50 (0.037)	0.5560	$A_3B_2C_1D_3E_2$
24	150	150	15	0.50 (0.037)	0.6672	$A_3B_2C_1D_3E_3$
25	150	200	20	0.40 (0.090)	0.4448	$A_3B_3C_2D_1E_1$
26	150	200	20	0.40 (0.090)	0.5560	$A_3B_3C_2D_1E_2$
27	150	200	20	0.40 (0.090)	0.6672	$A_3B_3C_2D_1E_3$

three levels (Table 1). According to the performance and parameter requirements of automatic plastering machines, the maximum nozzle length is set to be 150 mm, the thickness cannot exceed 25 mm, the water-cement ratio should be set in a range of 0.4 to 0.5 (a different water-cement ratio corresponds to a different dynamic viscosity), and the nozzle inlet velocity can be set as 0.556 m/s ± 20%.

For this experiment of five factors with three levels each, an L_{27} orthogonal array is an appropriate design for conduct the experiment, as shown in Table 2.

3.2 Simulation preparation

The finite volume method, also known as the control volume integral method, is developed on the basis of the finite difference method. Similar to the finite element method, the finite volume method divides the solution domain into discrete grids of limited size. For each grid node, the node control volume is formed in the way of surrounding the node. The key step is the integral of the control differential equations in the control volume [19]. One of the popular software for the finite volume method is ANSYS Fluent, a computational fluid-dynamics software. Before using ANSYS Fluent, we need to conduct the simulation preparation by setting the boundary conditions and building the 3D mesh model.

It is known that the maximum flow of pump supply is 4 m^3/h, the inlet velocity is 0.556 m/s, and the mortar density is 1700 kg/m^3. It can be shown that the nozzle flow field is in a laminar flow state by calculating its Reynolds number. Boundary conditions of the nozzle inlet are set as the boundary conditions of velocity inlet, while the boundary conditions of the nozzle outlet are set as free flow. The pressure and velocity coupling algorithm is used as the solver, where the gravity is ignored. Other parameters are set as default values of the software. The nozzles with different sizes are simulated by ANSYS Fluent simulation software with these boundary conditions.

The 3D mesh model of the nozzle is built by the GAMBIT software, whose geometry is mainly divided into tetrahedron meshes, including hexahedron, conical, and woven meshes in certain locations [20–23]. The 3D mesh model of the nozzle is shown in Fig. 2. The coordinate directions of the model are set as follows: the direction of mortar spraying is set as x-direction; the direction of the gravity is set as the z-direction. In the simulation, we mainly study the outlet velocity uniformity in the x-direction and the distributions of velocity on the plane ($z = 0$).

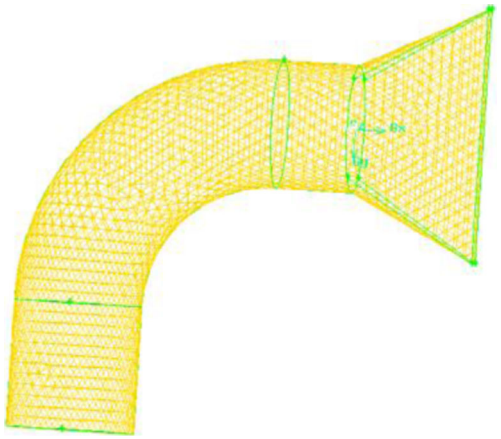

Fig. 2 3D mesh model of the nozzle

4 Results and analysis

4.1 Results of ANSYS fluent simulation

We input the boundary conditions and the 3D mesh model of the nozzle into ANSYS Fluent and conduct the simulation for the 27 tests specified in the L_{27} orthogonal array in Table 2. For each of the 27 tests, we can get the outlet velocity curve in the x-direction (Fig. 3) and the distributions of velocity on the plane of $z = 0$ (Fig. 4).

As can be seen in Figs. 3 and 4, the variations of inlet velocity have only a minimum impact on the curve chart (Fig. 3) and the cloud chart (Fig. 4) when other factors are unchanged. When the nozzle length is unchanged, the outlet velocity of the nozzle shows different degrees of fluctuation with the increase of the nozzle width. The velocity distribution of the internal flow field becomes non-uniformity. Test 7, Test 8, and Test 9 show the back flow phenomenon because the width of the nozzle is relatively wide (200 mm) when the length is short (50 mm). This situation improves with the increase of the nozzle length, i.e., the sudden increase of the flow channel width can make the flow field unstable. Further analysis can be done on the experimental data using Minitab statistical software.

4.2 Results of orthogonal tests

The velocity of each element center at the x-direction of the nozzle outlet (the vertical direction to the wall) for each of the 27 tests is shown in Table 3. The data are imported from ANSYS Fluent into Minitab software for calculating the outlet velocity variance for each test and

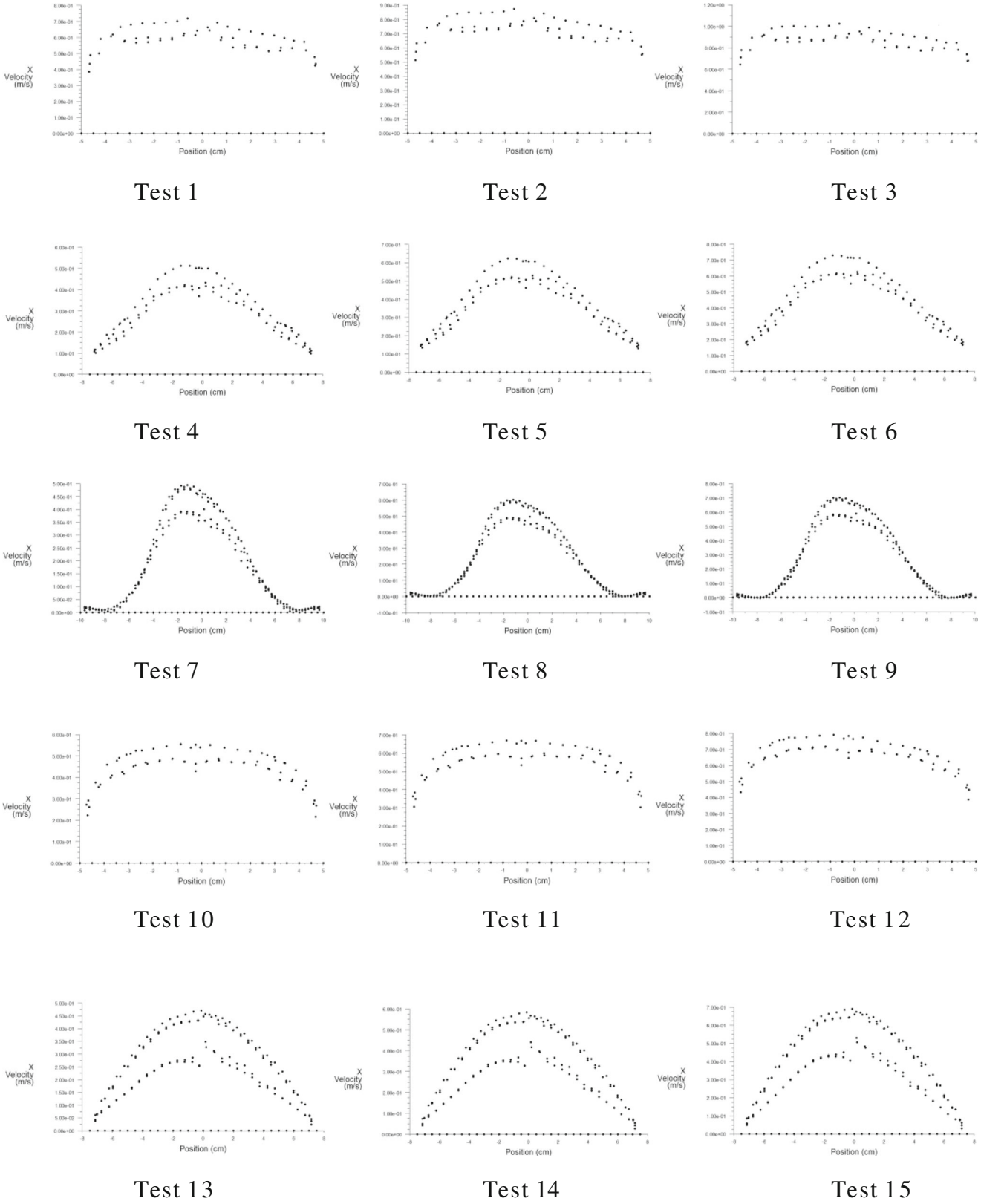

Fig. 3 The outlet velocity curve of *x*-direction

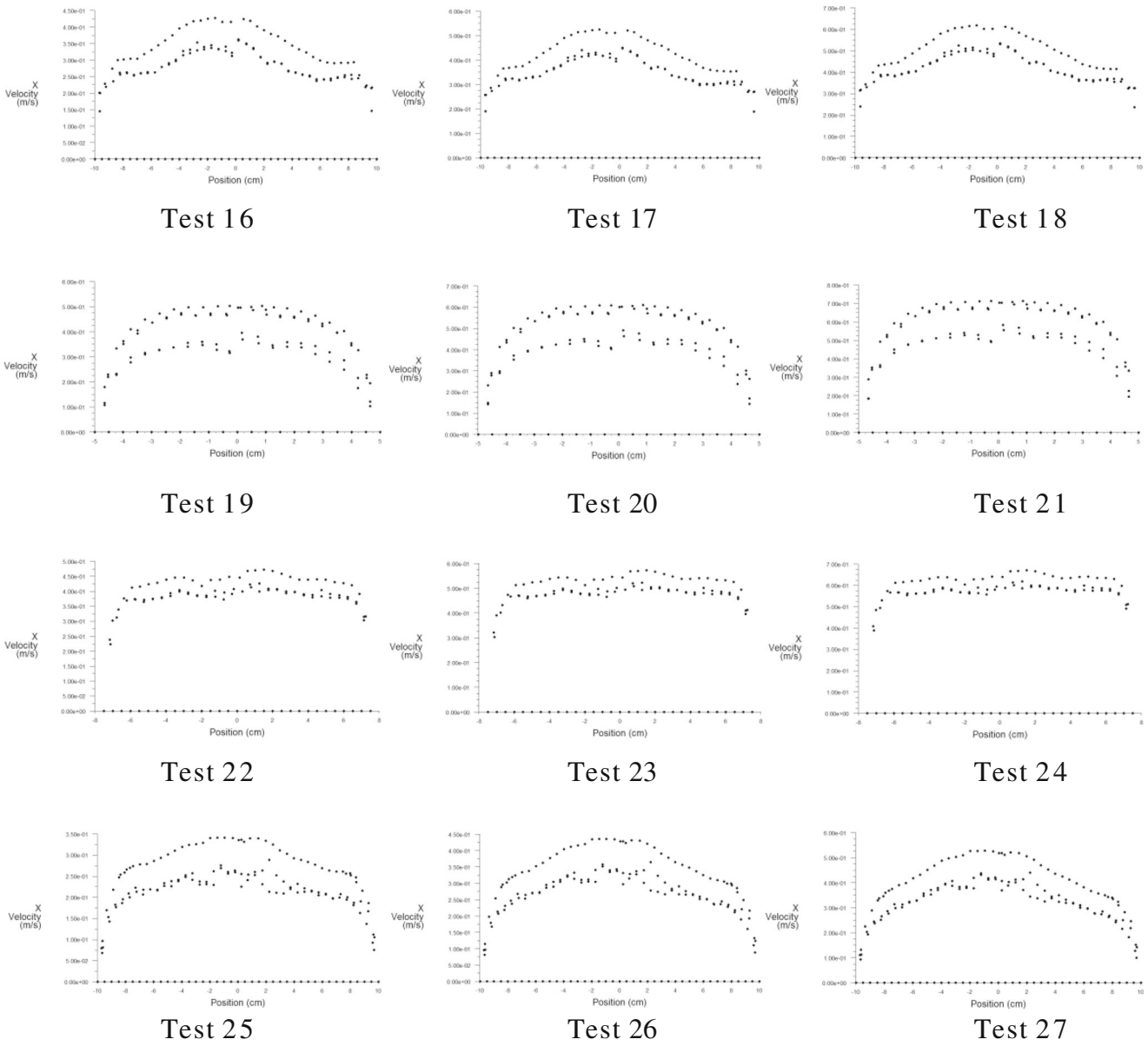

Fig. 3 (continued)

further analysis. The analysis results are shown in Fig. 5, with the SN ratio responses (left) and the mean responses (right); Fig. 6 shows the main effect of SN ratios (left) and the main effect of the mean (right); and Fig. 7 presents the interaction of outlet velocity variances.

4.3 Analysis of results

In the analysis of multifactor experiments, the main goal is to investigate whether the independent variables (factors) have the main effects and interaction effects. The main effect is the effect of a single independent variable on a dependent variable, when all the other independent variables are unchanged []. Two independent variables interact if the effect of one of the variables differs depending on the level of the other variable. If the effect of an independent variable on the dependent variable varies according to the level of another independent variable, we can say that there is an interaction effect between the two independent variables.

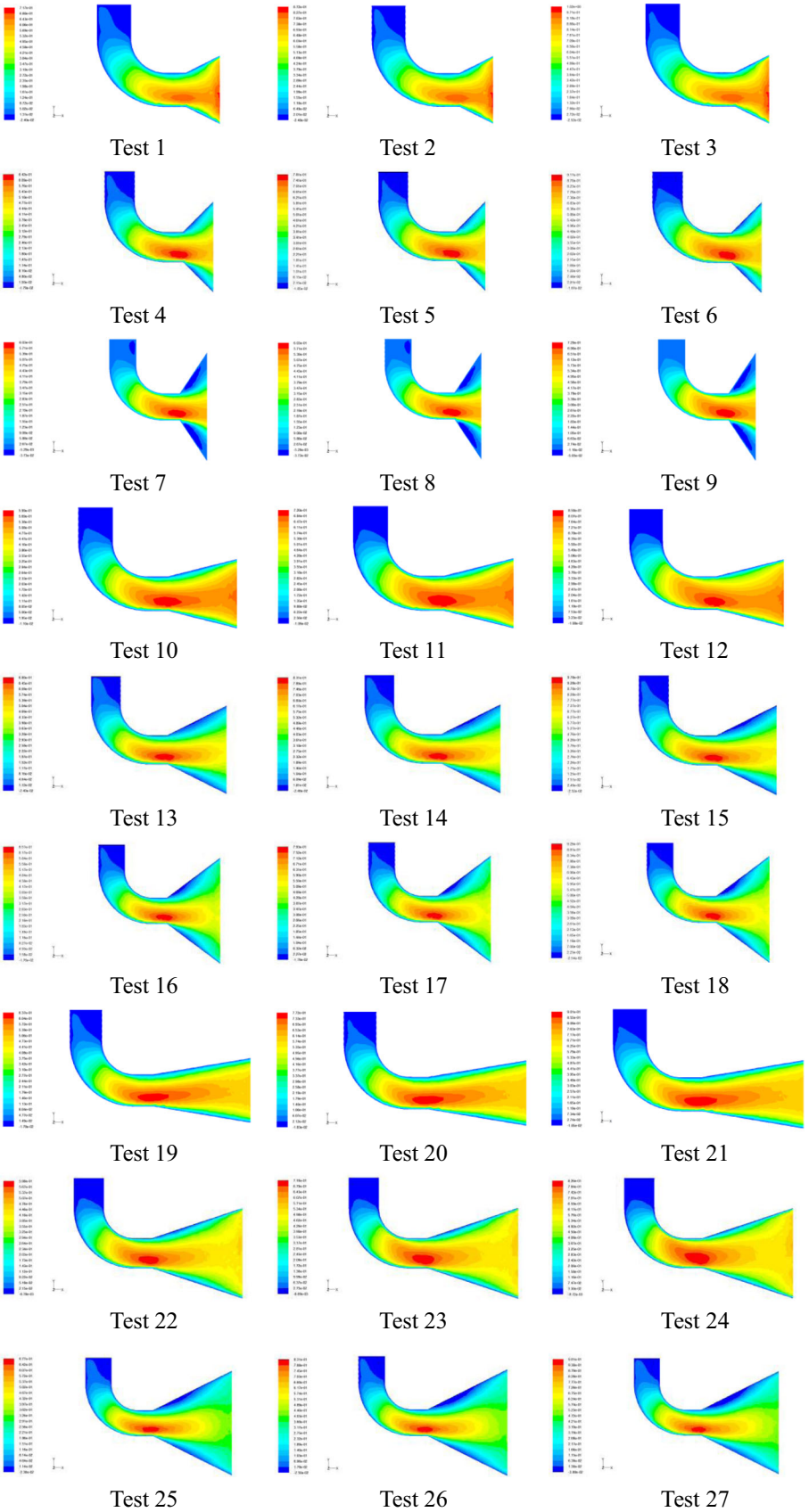

Fig. 4 The distributions of velocity on the plane $z = 0$

Table 3 Orthogonal test results

No.	Factor					Outlet velocity variance
	Length A (mm)	Width B (mm)	Thickness C (mm)	Water cement ratio D (dynamic viscosity Pa·s)	Inlet velocity (m/s)	
1	50	100	15	0.40 (0.090)	0.4448	0.1263
2	50	100	15	0.40 (0.090)	0.5560	0.1393
3	50	100	15	0.40 (0.090)	0.6672	0.1502
4	50	150	20	0.45 (0.063)	0.4448	0.1291
5	50	150	20	0.45 (0.063)	0.5560	0.1536
6	50	150	20	0.45 (0.063)	0.6672	0.1764
7	50	200	25	0.50 (0.037)	0.4448	0.1625
8	50	200	25	0.50 (0.037)	0.5560	0.2031
9	50	200	25	0.50 (0.037)	0.6672	0.2422
10	100	100	20	0.50 (0.037)	0.4448	0.1016
11	100	100	20	0.50 (0.037)	0.5560	0.1105
12	100	100	20	0.50 (0.037)	0.6672	0.1139
13	100	150	25	0.40 (0.090)	0.4448	0.1425
14	100	150	25	0.40 (0.090)	0.5560	0.1768
15	100	150	25	0.40 (0.090)	0.6672	0.1263
16	100	200	15	0.45 (0.063)	0.4448	0.0875
17	100	200	15	0.45 (0.063)	0.5560	0.1018
18	100	200	15	0.45 (0.063)	0.6672	0.1142
19	150	100	25	0.45 (0.063)	0.4448	0.1269
20	150	100	25	0.45 (0.063)	0.5560	0.1461
21	150	100	25	0.45 (0.063)	0.6672	0.1621
22	150	150	15	0.50 (0.037)	0.4448	0.0671
23	150	150	15	0.50 (0.037)	0.5560	0.0720
24	150	150	15	0.50 (0.037)	0.6672	0.0752
25	150	200	20	0.40 (0.090)	0.4448	0.0916
26	150	200	20	0.40 (0.090)	0.5560	0.1134
27	150	200	20	0.40 (0.090)	0.6672	0.1352

When there is no significant interaction effect between two independent variables, we can directly evaluate the role of the independent variable on the dependent variable from its main effect. When there is a significant interaction effect between two independent variables, we cannot simply draw conclusions directly from the main effects [24–26].

Figure 5 shows the influence degree of various factors (independent variables) on the outlet velocity variance (dependent variable): thickness (C) > length (A) > inlet velocity (E) >

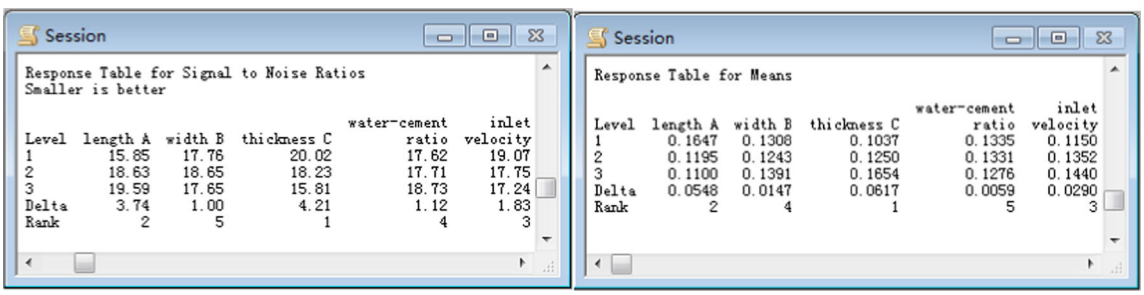

Fig. 5 SN ratio responses (*left*) and mean responses (*right*)

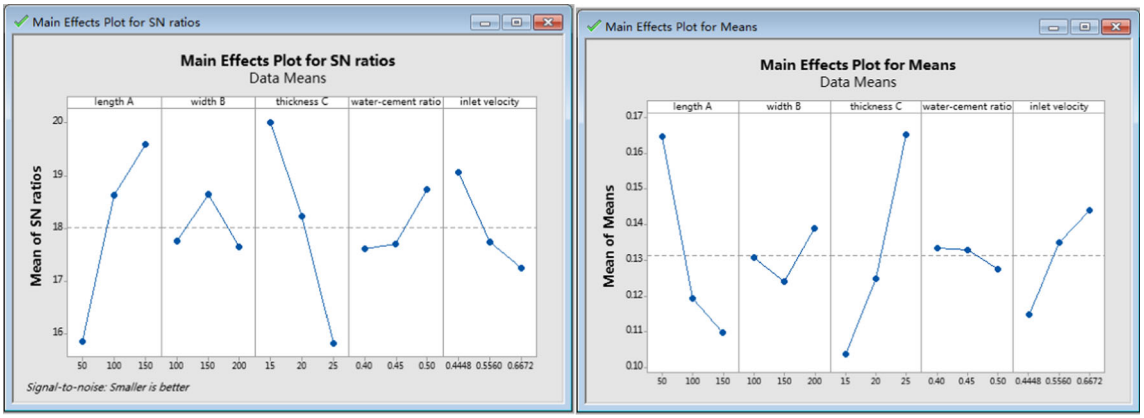

Fig. 6 Main effect of SN ratio (*left*) and main effect of mean (*right*)

width (B) > water-cement ratio (D). Figure 7 shows the significant interaction effects between length (A) and thickness (C), length (A) and width (B), and width (B) and thickness (C). Combining with the observations in Fig. 6, we can conclude that the optimal solution can be obtained when we take the factor levels of A3B2C1, namely, the nozzle length of 150 mm, the width of 150 mm, and the thickness of 15 mm. If the requirement of plastering quality and efficiency is satisfied, we can choose a higher water-cement ratio and a lower inlet velocity in order to minimize the outlet velocity variance (Fig. 5).

5 Conclusions

The research conducted in this paper optimizes the design of non-circular mortar nozzles for automatic wall-plastering machines by studying the effects of different parameters on the spray uniformity, especially the complex interaction effects of the nozzle structure parameters (the length, width, and thickness), the nozzle inlet velocity, and the water-cement ratio. The study is implemented using the orthogonal array in Taguchi methods and the finite volume method, realized in Minitab software and ANSYS Fluent software, respectively. The optimized structure parameters of non-circular nozzles can enhance the spraying uniformity with a larger spraying area, leading to a higher plastering quality and efficiency.

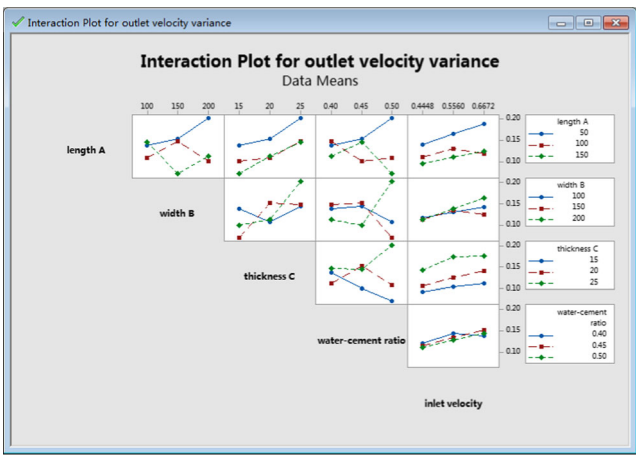

Fig. 7 Interaction of outlet velocity variances

The results from the optimal design of non-circular mortar nozzles indicate the following: (1) the factors' influence degree on the uniformity of nozzle outlet velocity is as follows: thickness (C) > length (A) > inlet velocity (E) > width (B) > water-cement ratio (D); (2) when the factor levels of A3B2C1 (the nozzle length of 150 mm, the width of 150 mm, and the thickness of 15 mm) is taken, the design scheme is the optimal, i.e., the variance of the outlet velocity is minimum considering the actual working conditions; and (3) a higher water-cement ratio and a lower inlet velocity should be chosen as long as it can meet the requirements of plastering quality and efficiency. The results provide an important reference for the systematic design of non-circular mortar nozzles in the future. This research can be extended to study additional design parameters, such as the mortar multiphase flow and the vibration of spraying machines for non-circular or other nozzle shapes.

Acknowledgements This study was supported by National Natural Science Foundation of China (NSFC) (Project Nos. 51375352 and 7127116) and Teaching Research Project of Hubei Province (Project No. 2014237) in China.

References

1. Liu Y, Zhao J, Kong X (2004) The design of pneumatics system for half-automatic plastering machine [J]. Machine Tool & Hydraulics 11:107–107. doi:10.3969/j.issn.1001-3881.2004.11.040
2. Wang Y, Xie S, Wang J (2012) Design and simulate on no-dead-corner plastering machine [J]. Journal of Southwest China Normal University (Natural Science Edition) 37(11):112–115. doi:10.3969/j.issn.1000-5471.2012.11.022
3. L. Lu, C. Chen (2013) Design of a new type of automatic plastering machine [J]. Mech Eng Autom (5)91. doi:10.3969/j.issn.1672–6413.2013.05.037
4. Long T, Li E, Fang Z (2015) Type of intelligent wall plastering machine and research progress of its key technologies [J]. Journal

of Shandong Jianzhu University 1:65–70. doi:10.3969/j.issn.1673-7644.2015.01.012
5. Ma F, Zhang W (2006) Numerical simulation on internal flow field in a bore-enlarged nozzle with water jet [J]. Journal of Beijing University of Science And Technology 28(6):576–580. doi:10.3321/j.issn:1001-053X.2006.06.015
6. Yuan S, Wei Y, Li H (2010) Structure design and experiments on the water distribution of the variable-rate sprinkler with non-circle nozzle [J]. Transactions of The Chinese Society of Agricultural Engineering 26(9):149–153. doi:10.3969/j.issn.1002-6819.2010.09.025
7. Kim JH, Kim HD, Setoguchi T (2010) The effect of diffuser angle on the discharge coefficient of a miniature critical nozzle [J]. J Therm Sci 19(3):222–227
8. Long X, Han N, Chen Q (2008) Influence of nozzle exit tip thickness on the performance and flow field of jet pump [J]. Journal of Mechanical Science & Technology 22(10):1959–1965
9. Chen G, Wu C, Shen J (2010) Numerical simulation of flow field of auxiliary nozzle as affected by orifice forms of air-jet loom based on fluent [J]. Journal of Textile Research 31(8):122–124
10. Wo H, Yao Z, Wang G (2011) Numerical simulation of cavitation now in engine nozzle [J]. Journal of Hefei University of Technology 34(5):651–654
11. Wang D, Dan Q, Liu M (2012) Research on characteristics of fluid flow in wavy channel based on lagrange tracking method [J]. J Eng Thermophys 33(3):481–484
12. Zhang W, Lin Y, Chen P (2011) Numerical simulation of ice accretion and parameter effects based on Eulerian droplet model [J]. Journal of Nanjing University of Aeronautics & Astronautics 43(3):375–380
13. Zhu H, Lin Y, Xie L (2010) Fluent fluid analysis and simulation practical tutorial [M]. People Post Press. doi:10.1134/S1063778810080016
14. Lei T, J (1998) New Compilation of Hydraulic Engineering Manual. Beijing Institute of Technology Press, Beijing, China, 313–318
15. Zuo H, Bai L, Zhou J (2013) Visualization research on the internal flow field of non-circle nozzle [J]. Journal of Hunan University of Technology 27(1):43–47. doi:10.3969/j.issn.1673-9833.2013.01.010
16. Wen X, Zhang G (2015) Design and simulation based on fluent for fire fighting bubble atomizer [J]. Chinese Hydraulics & Pneumatics 4:47–49. doi:10.11832/j.issn.1000-4858.2015.04.010
17. Liu P, Liao X, Cheng W et al (2015) Design of Streamline Nozzle Height of fire monitor based on fluent [J]. Machine Tool & Hydraulics 1:99–102. doi:10.3969/j.issn.1001-3881.2015.01.025
18. Hascalık A, Caydas U (2008) Optimization of turning parameters for surface roughness and tool life based on the Taguchi method [J]. Int J Adv Manuf Technol 38:896–903
19. Li R, X (2005) Finite volume method. *National Defense Industry Press, Beijing, China.(In Chinese)*
20. Y. Gong, C. Guo, J. Hou (2014) Full-size structure optimization based on fluent about pulse jet nozzle [J]. Hydraul Pneum (11)
21. Zhou Z, Ma D (2010) Numerical simulation of high-pressure jet nozzle based on fluent [J]. Machine Building & Automation 39(1):61–62. doi:10.3969/j.issn.1671-5276.2010.01.021
22. Dang J, Luo K, Zhang Y et al (2005) Design and test research of big flux adjustable atomizer nozzle [J]. Machine Tool & Hydraulics 9:72–74. doi:10.3969/j.issn.1001-3881.2005.09.029
23. Yong L, You L (2001) A brief introduction to fluent—a general purpose CFD code [J]. J Hydrodyn 16(2):254–258. doi:10.3969/j.issn.1000-4874.2001.02.017
24. Bement TR (1989) Taguchi techniques for quality engineering [J]. Technimetrics 31(2):253–255
25. H. Garg, V. Karar, R. Kumar (2013) Optimization design of microchannel heat sink based on Taguchi method and simulation [C]. Sci Inform Conf IEEE 166–170
26. Palanikumar K (2008) Application of Taguchi and response surface methodologies for surface roughness in machining glass fiber reinforced plastics by PCD tooling [J]. Int J Adv Manuf Technol 36(1–2):19–27